



Tropical climate-vegetation-fire relationships: multivariate evaluation of the land surface model JSBACH

Gitta Lasslop^{1,2}, Thomas Moeller¹, Donatella D'Onofrio³, Stijn Hantson⁴, and Silvia Kloster¹

¹Max-Planck Institute for Meteorology, Bundesstraße 53, 20146 Hamburg, Germany

²Senckenberg Biodiversity and Climate Research Centre, Senckenberganlage 25, 60325 Frankfurt am Main, Germany

³Institute of Atmospheric Sciences and Climate (ISAC-CNR), Torino, Italy

⁴Karlsruhe Institute of Technology, Institute of Meteorology and Climate research, Atmospheric Environmental Research, 82467 Garmisch-Partenkirchen, Germany

Correspondence: Gitta Lasslop (gitta.lasslop@senckenberg.de)

Abstract. The interactions between climate, vegetation and fire can strongly influence the future trajectories of vegetation in Earth system models. We evaluate the relationships between tropical climate, vegetation and fire in the global vegetation model JSBACH, using a simple fire scheme and the complex fire model SPITFIRE with the aim to identify potential for model improvement. We use two remote sensing products (based on MODIS and Landsat) in different resolutions to assess the robustness of the obtained observed relationships. We evaluate the model using a multivariate comparison that allows to focus on the interactions between climate, vegetation and fire and test the influence of land use change on the modelled patterns. Climate-vegetation-fire relationships are known to differ between continents we therefore perform the analysis for each continent separately.

The observed relationships are similar in the two satellite datasets, but maximum tree cover is reached at higher precipitation values for coarser resolution. The model captures the broad spatial patterns with regional differences, which are partly due to the climate forcing derived from an Earth system model. SPITFIRE strongly improves the spatial pattern of burned area and the distribution of burned area along increasing precipitation compared to the simple fire scheme. Surprisingly the correlation between precipitation and tree cover is higher in the observations than in the largely climate driven vegetation model, with both fire models. The multivariate comparison identifies a too high tree cover in low precipitation areas and a too strong relationship between high fire occurrence and low tree cover for the complex fire model. We therefore suggest that drought effects on tree cover and the impact of burned area on tree cover or the adaptation of trees to fire can be improved. The model reproduces the linear increase of tree cover with increasing precipitation for Australia, compared to the sigmoid increase for the other continents. As we find this linear increase for both fire models as well as for present day and preindustrial land use, we conclude that it appears in the model due to differences in climate not captured by mean annual precipitation. Land use contributes to the intercontinental differences in fire regimes with SPITFIRE and strongly overprints the modelled multimodality of tree cover with SPITFIRE. The multivariate comparison between observations and model used here has several advantages: it improves the attribution of model-data mismatches to model processes, it reduces the impact of biases in the meteorological forcing on the evaluation and it allows to evaluate not only a specific target variable but also the interactions.



Copyright statement.

1 Introduction

Capturing the interactions of vegetation cover and composition with the climatic drivers and related disturbances in Earth system models is crucial to provide reliable changes of vegetation for a changing climate. Climate is the main driver of global
5 vegetation patterns, but also vegetation has crucial impacts on the Earth system, due to its influence on the surface albedo and the water cycle (Bonan, 2008; Brovkin et al., 2009). The importance of vegetation type has been assessed in various studies: when compared to grasslands, forests in tropical areas cool the climate due to higher evapotranspiration while in boreal regions, forests warm the climate due to a reduction of the albedo (Bathiany et al., 2010). The relevance of vegetation also shows when
10 contrasting vegetated and non-vegetated surfaces: in the Sahel region this difference is of major importance for the climatic conditions (Brovkin et al., 1998).

Interactions between vegetation, fire and climate are particularly important to understand the spatial patterns in tropical vegetation, which is characterized by strong gradients from deserts to tropical rainforests. Remotely sensed tropical tree cover shows a bimodality between forest ($T > 60\%$) and savanna ($T < 60\%$) states for grid cells with similar climate. Intermediate tree cover
15 fractions (e.g. 60%) are virtually absent (Hirota et al., 2011; Staver et al., 2011b). The occurrence of this “gap” in tree cover was suggested to be caused by a feedback between fire and vegetation. Although the reliability of remotely sensed tree cover sets to diagnose this “gap” was recently questioned (Gerard et al., 2017), the bimodality in the distribution is also confirmed by canopy height (Xu et al., 2016) or biomass (Yin et al., 2014). The occurrence of both forest and savanna states under similar climate
20 conditions due to a feedback between fire and vegetation is supported by conceptual (Staver et al., 2011a) and process-based models (Higgins and Scheiter, 2012; Moncrieff et al., 2014; Lasslop et al., 2016).

While data analysis can provide insights on driving factors for certain variables, process-based models summarize the process
25 understanding and allow us to perform experiments that are impossible in reality. Dynamic global vegetation models (DGVMs) were developed to understand ecosystem dynamics, the carbon cycle and biosphere-atmosphere interactions (Sitch et al., 2003). Many of them are part of Earth system models (ESMs), to represent the dynamics of the land surface within the climate system. It is therefore important that DGVMs include appropriate representations of vegetation to obtain reliable simulations of the
30 Earth system (e.g. Baudena et al., 2015).

The development of remotely sensed global burned area products triggered the development of complex fire models within
DGVMs (Hantson et al., 2016). Over the recent years these models were applied to address the impact of fire on the carbon cycle (Li et al., 2014; Yue et al., 2016), the land surface temperature (Li et al., 2017) or the sensitivity of the fire model to driving
35 factors (Kloster et al., 2010; Lasslop and Kloster, 2015). Evaluation of fire models mostly focused on evaluating the burned area and carbon emissions, but also the importance of benchmarking effects on vegetation has been noted (Hantson et al., 2016). The evaluation, however, is based on comparing variables one by one and not the relationships between them. (Baudena et al., 2015) go beyond the geographic comparison by analyzing the relationship between tree cover and the main climatic
40 driver (precipitation). Also the relationship between precipitation and climate was evaluated in previous studies (Prentice et al.,



2011). However, to our knowledge, climate, vegetation and fire have not been combined in a multivariate model-observation comparison.

Here, we aim 1) to assess the robustness of observed climate-vegetation-fire relationships across the tropical continents based on two remotely sensed tree cover datasets; 2) to test a multivariate model evaluation to identify opportunities for model improvements in JSBACH, the vegetation model used within the MPI Earth system model, and 3) to test the contribution of land use change on the obtained relationships.

2 Model and Data

To investigate the climate-fire-vegetation relationships in the tropical regions we represent climate by the mean annual precipitation (P), vegetation by the tree (TC), grass (GC) and non-vegetated cover and fire as the burned fraction (BF).

We define the tropical region as between -30° and 30° latitude. As continental limits we chose -20° to 60° longitude and -30° to 30° latitude for Africa, 230° to 330° longitude and -30° to 30° latitude for South America, 60° to 160° longitude and -10° to 30° latitude for Asia and 100° to 160° longitude and -30° to -10° latitude for Australia.

2.1 Model and simulation description

We use the JSBACH land surface model (Reick et al., 2013), which is the land component of the MPI Earth system model (MPI-ESM) (Giorgetta et al., 2013). JSBACH simulates the terrestrial carbon and water cycle in a process based way. We use two fire algorithms, a simple empirical model (Brovkin et al., 2009; Reick et al., 2013) and the process-based fire model SPITFIRE (Lasslop et al., 2014). Results referring to simulations with the complex SPITFIRE model are referred to as JSBACH-SPITFIRE, simulations with the simple JSBACH standard fire scheme are indicated as JSBACH-standard. These two approaches span the range of complexity of currently used global scale fire models (Hantson et al., 2016). The JSBACH-standard fire computes burned area based on a minimum burned fraction which increases as a function of the litter carbon pools and relative humidity. SPITFIRE computes burned area based on human and lightning ignitions, fire spread rate and a fire duration. SPITFIRE distinguishes between different fuel particle sizes and uses a combination of minimum and maximum temperature, precipitation and soil moisture to determine the fuel moisture. Both fire models interact with the vegetation model as follows: JSBACH provides fuel amounts, vegetation composition and soil moisture as inputs to the fire model. The fire model in turn reduces the carbon pools of JSBACH according to the simulated carbon combustion of vegetation fires and reduces the cover fractions of burned vegetation. In the JSBACH-standard fire scheme the burned area directly translates into a reduction of the cover fractions of the plant functional types (PFTs), while in SPITFIRE the mortality of woody vegetation depends on the fire intensity, fire residence time, the vegetation height and bark thickness. The model's plant functional types for the tropics include C3 and C4 grass, tropical evergreen and deciduous trees, and rain green shrubs. Shrubs and trees compete according to their net primary productivity. Grasses and shrubs have an advantage compared to trees in regions with disturbances due to their lower establishment time scale (Reick et al., 2013, grasses: 1 year, shrubs: 12 years, tropical trees: 30 years). PFTs do not establish if the 5 years running mean net primary productivity (NPP) turns negative. Land use is included following



the protocol of Hurtt et al. (2011). The implementation is described in detail in (Reick et al., 2013). Croplands are excluded from fire occurrence while pastures are treated as natural grasslands with a higher fuel bulk density within SPITFIRE (Rabin et al., 2017). The JSBACH-standard fire excludes fire occurrence on both anthropogenic land cover types. JSBACH-SPITFIRE shows a reasonable agreement with remotely sensed data products for present day burned area and carbon emissions for simulations with prescribed land cover (Lasslop et al., 2014). The present setup with dynamic biogeography has been evaluated along the human dimensions population density and cropland fraction. The model tends to overestimate burned fraction for high cropland fractions and underestimates burned fraction for very low and high population densities (Lasslop and Kloster, 2017).

2.1.1 Simulation setup

JSBACH was forced with meteorological data extracted from a coupled simulation with the MPI-ESM version 1.1 for the historical period 1850-2005. The SPITFIRE model additionally uses a population density dataset (Klein Goldewijk et al., 2001) with decadal resolution and a monthly lightning climatology (LIS/OTD product of the LIS/OTD Science Team, <http://ghrc.msfc.nasa.gov>) as input for the computation of ignitions. The model's spatial resolution is $1.875^\circ \times 1.875^\circ$. The time step for plant productivity and hydrology is 30 minutes, while the disturbance routine is called once per day. During the 1000 year spinup period the first 28 years of forcing (1850-1877) were recycled and CO₂ concentration fixed at the value of 1850 (284.725 ppm). The subsequent transient historical simulation (Hist) from 1850-2005 accounts for the changes in atmospheric CO₂, climate, population density and land use. A complementary simulation accounting only for the rise in atmospheric CO₂, transient climate and population density but using the land use of 1850 for the whole period (cLU) is used to isolate the effect of land use change on the climate - vegetation - fire relationships. When comparing the model output to observations, the averaging period for the model simulations was 1996-2005, as the forcing was only available until 2005.

2.2 Datasets for model evaluation

We averaged the remote sensing datasets over the years that were covered by all datasets (2001-2010). Model output is only available until the year 2005. Using only the overlapping period (2001-2005) would decrease the robustness of the mean fire regime and climate characterization. We therefore use different averaging periods for model (1996-2005) and observations (2001-2010). The presentation of the relationship between precipitation, tree cover and burned fraction based on remote sensing data is based on 0.25° resolution and for the comparison with the model the datasets were aggregated to the model resolution ($1.875^\circ \times 1.875^\circ$).

2.2.1 Vegetation and land cover

We use two tree cover datasets based on satellite data, one based on the MODIS (moderate-resolution imaging spectroradiometer) sensor (Townsend et al., 2011), the other on the Landsat satellite (Hansen et al., 2013). Additionally we use the non-tree vegetation cover and non-vegetation cover of the MOD44B product version 051 (downloaded 6/February 2017, using the R



modis package).

The maximum tree cover in the MODIS dataset is 80%. This however corresponds to 100% crown cover (Hansen et al., 2003). The modelled cover fractions represent rather the crown cover with a 100% maximum, we therefore linearly rescaled the tree cover data to improve the consistency between model and observations. The second dataset based on Landsat data builds on a high spatial resolution of 30m (Hansen et al., 2013). The dataset provides annual forest gain and loss over the period from 2000-2012. Alkama and Cescatti (2016) reconstructed the annual tree cover and aggregated the dataset to 0.05°. Here, we used the mean over their reconstructed annual tree cover values from 2001-2010.

The MODIS collection 5 land cover dataset (Friedl et al., 2010) was used to test the influence of shrub lands (open and closed shrub lands), as the tree cover data have a higher uncertainty for shrublands. The filtering was applied on 0.05° spatial resolution. This dataset is distributed by the Land Processes Distributed Active Archive Center (LP DAAC), located at the U.S. Geological Survey (USGS) Earth Resources Observation and Science (EROS) Center (lpdaac.usgs.gov), distributed in netCDF format by the Integrated Climate Data Center (ICDC, <http://icdc.cen.uni-hamburg.de>) University of Hamburg, Hamburg, Germany in 0.05° spatial resolution and annual time step.

2.2.2 Fire

The global fire emissions database (GFED, <http://www.globalfiredata.org/>) provides globally gridded monthly burned area based on the MODIS sensor. We used the version 4 of the dataset (Giglio et al., 2013).

2.2.3 Precipitation

The “TRMM and Other Data Precipitation Data Set” (TMPA) is based on the Version 7 TRMM Multi-satellite Precipitation Analysis algorithm (Huffman et al., 2007, 2010). The product has near global coverage from 50° north to 50° south. The precipitation estimate (including rain, drizzle, snow, graupel and hail) is based on a combination of multiple data sources including precipitation gauges. The dataset is available online (http://disc.sci.gsfc.nasa.gov/gesNews/trmm_v7_multisat_precip).

3 Results

3.1 Spatial distribution of vegetation cover, area burnt and precipitation in the tropics

The two observational satellite based tree cover datasets are consistent and show only small differences in their spatial pattern (Figure 1a). The overall clear pattern in tree cover is a transition from very high tree cover in moist rain forest regions to low tree cover in the drier savannas to the absence of trees in the desert regions. Both models reproduce this overall observed pattern, although with marked local differences. Both model versions overestimate tree cover in northern Australia to a similar extent. In the North-Eastern Amazon region the simulations underestimate tree cover compared to the observations. This underestimation is much smaller for JSBACH-SPITFIRE. The simulations overestimate tree cover in Southern Hemisphere Africa, this overestimation is again smaller for JSBACH-SPITFIRE. The simulated grass cover has higher maximum values,



but generally is often lower than observed by satellite (Figure 1 d). The non-vegetated fraction is captured well by the models (Figure 1 e).

Generally JSBACH-standard strongly underestimates the total area burnt and the spatial variability (Figure 1 b). JSBACH-SPITFIRE improves the capability to represent fire regimes with high fire occurrences. The tropical average burned area per year is for JSBACH-standard 65 Mha, for JSBACH-SPITFIRE 242 Mha and for the satellite dataset 315 Mha. In South America spatial patterns in JSBACH-standard are inconsistent with the observations (most burning in the Northeast). JSBACH-SPITFIRE overestimates fire occurrence in South America but the spatial patterns are more similar to observations. In Africa we find reasonable agreement between JSBACH-SPITFIRE and the observations. JSBACH-standard shows a strong underestimation of the burned fraction (max. 10% of the grid cell area year⁻¹, while the observations show up to 100%). In Australia JSBACH-SPITFIRE and JSBACH-standard show similar patterns and both strongly underestimate the burned area.

Precipitation of the MPI-ESM forcing shows a dry bias in the East and central Amazon region, a dry bias in Asia, and moister conditions in the western part of southern hemisphere Africa (Figure 1 c). The dry bias in South America and Asia is known from previous ECHAM model versions (Hagemann et al., 2013; Stevens et al., 2013). The dry bias in precipitation in the Amazon may for instance explain the high bias in burned area in that region.

15

3.2 Climate-fire-vegetation relationships: comparison of observation datasets

Maximum tree cover shows an increase along the precipitation gradient across all continents, with trees being absent until a certain threshold (300-500 mm year⁻¹), increasing maximum tree cover and saturation of maximum tree cover for high precipitation (between 1500 and 2000 mm year⁻¹). The two remotely sensed tree cover datasets are consistent in their variation along the precipitation gradient (Figure 2). Fire occurrence is much higher for the African and Australian continent compared to South America and Asia. For tree cover fractions higher than 0.8, fire is virtually absent. Beyond this distinction there is no clear increase in burned fraction for decreasing tree cover at a given precipitation value. For Australia and Africa fire occurrence is very low below a mean annual precipitation of 300 mm year⁻¹, for South America and Asia already below 500 mm year⁻¹.

The Spearman rank correlation between precipitation and tree cover is very similar for both tree cover datasets (Table 1). The statistical precipitation thresholds for low (but higher than 0) and high tree cover differ by less than 100 mm. The aggregation to the model resolution shows the strongest effect on the precipitation threshold for high tree cover and shifts this value to higher precipitation. The association between precipitation and burned area is less sensitive to the aggregation: 80% of the global burned area occurs in regions with precipitation between 609 and 1518 mm on 0.25° resolution and between 635 and 1495 mm in 1.875° resolution.

30

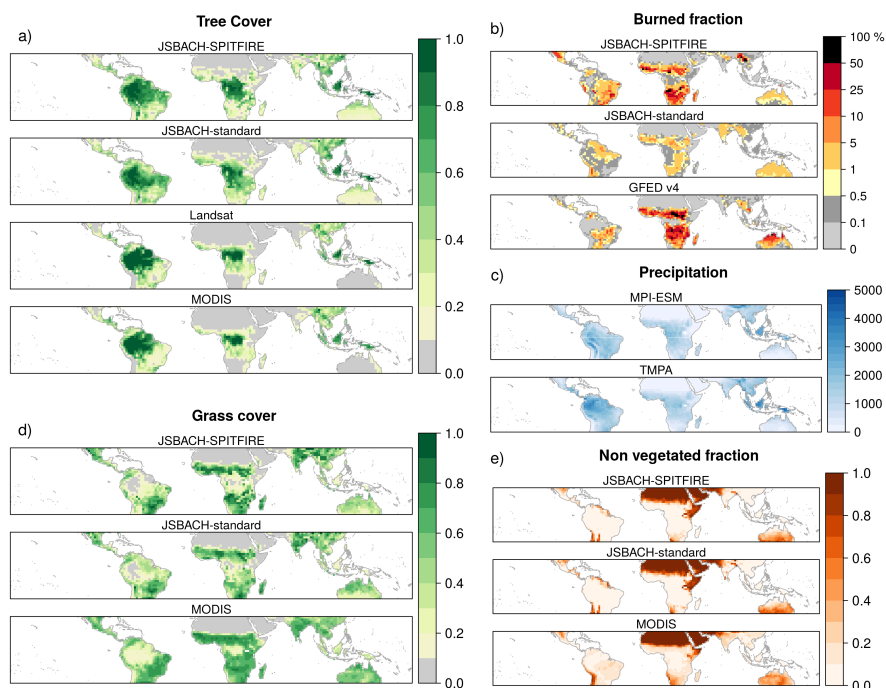


Figure 1. Spatial distribution of modelled and observed datasets used in this study. (a): Spatial distribution of tree cover fraction over the global tropics for the JSBACH-SPITFIRE and JSBACH-standard model simulation and the satellite data products from Landsat and MODIS. (b): Burned fraction [year^{-1}] as modeled by JSBACH-SPITFIRE and JSBACH-standard and the GFED v4 satellite product. (c): Precipitation in mm year^{-1} of the MPI-ESM and the TMPA dataset. (d): Grass cover fraction, and (e): non-vegetated fraction of the grid cell for the models and the MODIS satellite product. All datasets were remapped to the 1.875° model resolution.

3.3 Climate-fire-vegetation relationships: Evaluation of model results

In the tropics the observed burned area is strongly constrained by precipitation, around 80% of the burned area is observed in regions with mean annual precipitation between 600 and 1500 mm year^{-1} . This precipitation range is slightly larger for the model simulations (Table 1). JSBACH-SPITFIRE reproduces the increase in burned area for low precipitation, but slightly overestimates the contribution of grid cells with precipitation higher than ca. 1300 mm year^{-1} to the total burned area (Figure 3). JSBACH-standard overestimates the contribution of areas with low precipitation, but agrees well on the contribution of areas with high precipitation ($>1300 \text{ mm year}^{-1}$) when compared to the satellite observations.

Tree cover is overestimated for low precipitation values ($< 500 \text{ mm year}^{-1}$) in simulations with both fire models (Figure 4). Fire occurrence is limited in regions with low precipitation due to low fuel availability (Krawchuk and Moritz, 2011). This low fire occurrence is well reproduced by JSBACH-SPITFIRE and for most continents also by JSBACH-standard with the exception of Australia where the burned fraction of JSBACH-standard shows almost no variability. JSBACH-SPITFIRE has a stronger relationship between low tree cover and high fire occurrence than the observations. In JSBACH-SPITFIRE the highest

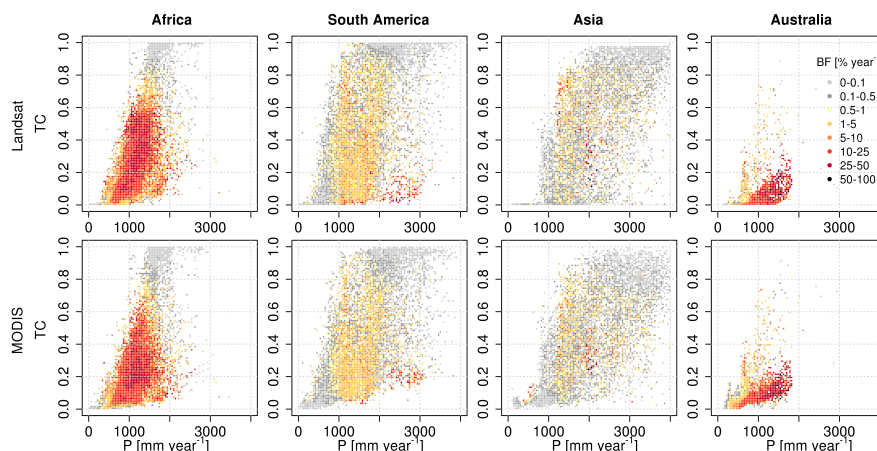


Figure 2. Tree cover (TC) versus precipitation [mm year^{-1}] with color coded burned fraction (BF) for different continents for the two satellite datasets. Burned area is averaged over data points with the same precipitation (40 mm steps) and tree cover (in steps of 0.01) to avoid over-plotting based on a spatial resolution of 0.25° . For Asia some higher precipitation values were cut off.

burned fractions ($> 50\%$ of grid cells year^{-1}) are found in Africa for the lowest tree covers (0.1) and for precipitation between $1000\text{--}2000 \text{ mm year}^{-1}$ (Figure 4). The observations show similar values of the burned fraction for tree cover values up to 0.3 for MODIS and up to 0.5 for LANDSAT. JSBACH-standard in many grid cells shows low fire occurrence for low tree cover, especially for South America, these grid cells have a high fraction of crops or pasture, which both are excluded from burning in JSBACH-standard (in SPITFIRE only crops are excluded). Burned fraction is much lower in Asia and South America compared to Australia and Africa in the observations. Both models show an underestimation of the fire occurrence in Australia. SPITFIRE reproduces the strong fire regime in Africa. In JSBACH-standard the difference in burned fraction between the continents is smaller than in JSBACH-SPITFIRE.

Models and observations show differences between continents in the relationship between precipitation and tree cover. For Australia maximum tree cover increases linearly with increasing precipitation for models and observations. For the other three continents in the observations the tree cover increase has a sigmoid shape with a saturation for high precipitation. For JSBACH-standard the increase in maximum tree cover is linear but also saturates, the increase in JSBACH-SPITFIRE more closely resembles the sigmoid shape of the satellite observations.

Surprisingly the observations show a higher Spearman correlation between tree cover and precipitation than the models (Table 1). The lower correlation of the modelled relationship most likely originates from the lower precipitation regions, where the maximum tree cover is very low in the observations and models strongly overestimate the maximum tree cover.

The grass cover has a much higher variability in the model compared to the MODIS data (Figure 5). The modelled non-vegetated fraction decreases faster with increasing precipitation compared to the observations (Figure 5). The dominance of trees (computed as $\text{TC}/\text{total vegetation cover}$) is strongly overestimated in the model for low precipitation ($< 500 \text{ mm year}^{-1}$,



Table 1. Spearman rank correlation (R) between precipitation (P) and tree cover (TC), required precipitation [mm year⁻¹] for 0.05 < TC < 0.15 and 0.85 < TC < 0.95, estimated as 0.05 quantile of precipitation for grid cells with the specific TC only, and precipitation value [mm year⁻¹] where 10% and 90% of the burned area (BA) originates from areas with lower precipitation. For the remote sensing datasets TMPA was used as precipitation, for the simulations (Hist, cLU, and JSBACH-standard) the MPI-ESM precipitation was used. Model results are all in 1.875° resolution.

Data	R(P,TC)	0.05 quantile of P for 0.05 < TC < 0.15	0.05 quantile of P for 0.85 < TC < 0.95	10% of BA has lower P	90% of BA has lower P
Landsat 0.25°	0.90	568	1417		
Landsat 1.875°	0.91	569	1596		
MODIS 0.25°	0.91	425	1514		
MODIS 1.875°	0.93	462	1644		
GFED v4 0.25°				607	1517
GFED v4 1.875°				635	1489
JSBACH-SPITFIRE Hist	0.79	31	1268	652	1663
JSBACH-SPITFIRE cLU	0.78	13	1000	700	1654
JSBACH-standard	0.87	34	1597	266	1519

Figure 5). While the relationship between precipitation and non-vegetated fraction is similar between the continents, the relationship for grass cover differs (Figure 5). For Australia observations and modelled grass cover increases with increasing precipitation. In Africa, South America and Asia grass cover first increases and then decreases with increasing precipitation.

5 3.4 Climate-fire-vegetation relationships: Influences of land use change

The simulation with land use of 1850 shows a strong gap between the savanna systems (TC < 40%) and closed forests (TC > 70%) for Africa and less strong for South America (Figure 6). For Australia and Asia the simulation does not show this pattern. For the historical simulation land use overprints this pattern of the natural vegetation dynamics. The difference in fire occurrence between Africa and South America is smaller for the simulation with preindustrial land use compared to the historical simulation (Figure 6 compared to Figure 4).

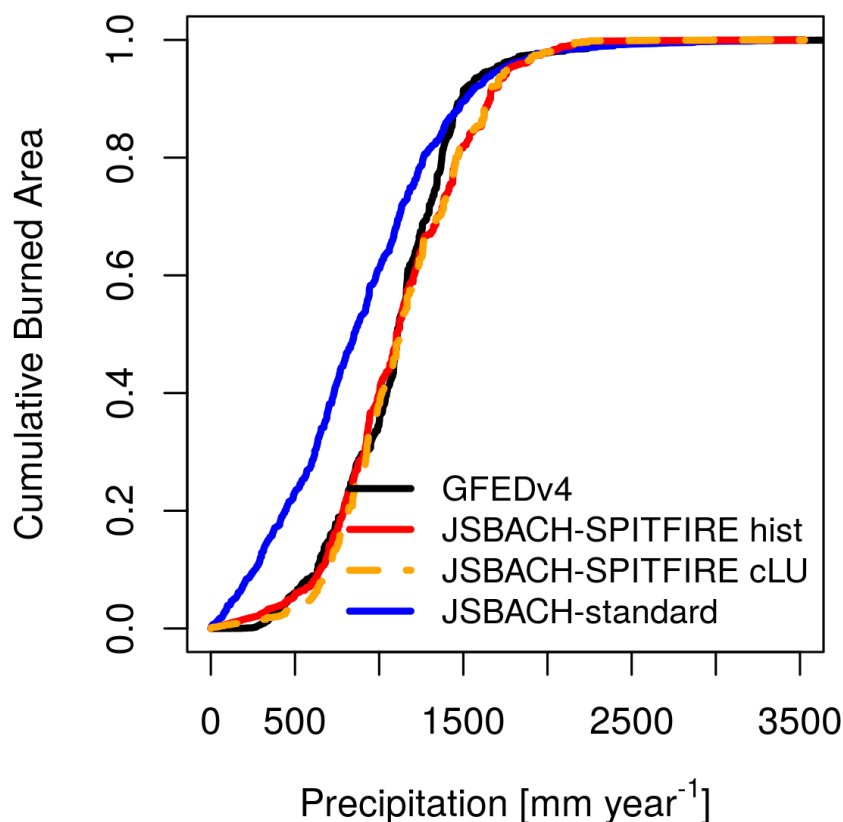


Figure 3. Cumulative burned area normalized with the total burned area for increasing precipitation. For the GFEDv4 burned area the TMPA dataset was used, for the model simulations the MPI-ESM precipitation was used.

4 Discussion

The multivariate model-data comparison identified differences and agreements between modelled and observed interactions between fire, vegetation and climate. It goes beyond spatial comparisons by providing better guidance on which processes in the model need improvement. We here discuss which model improvements can help to address the differences, what causes
5 agreements in intercontinental differences and whether limitations of the observations might influence our findings.

4.1 Opportunities for model improvements

JSBACH overestimates tree cover for low precipitation on all tropical continents. In these dry regions no or only very low burned fractions are observed, and the fire models show a good response to precipitation (Figure 3). Improvements in the fire model can therefore not improve this mismatch. The productivity of vegetation in the JSBACH model depends on the avail-

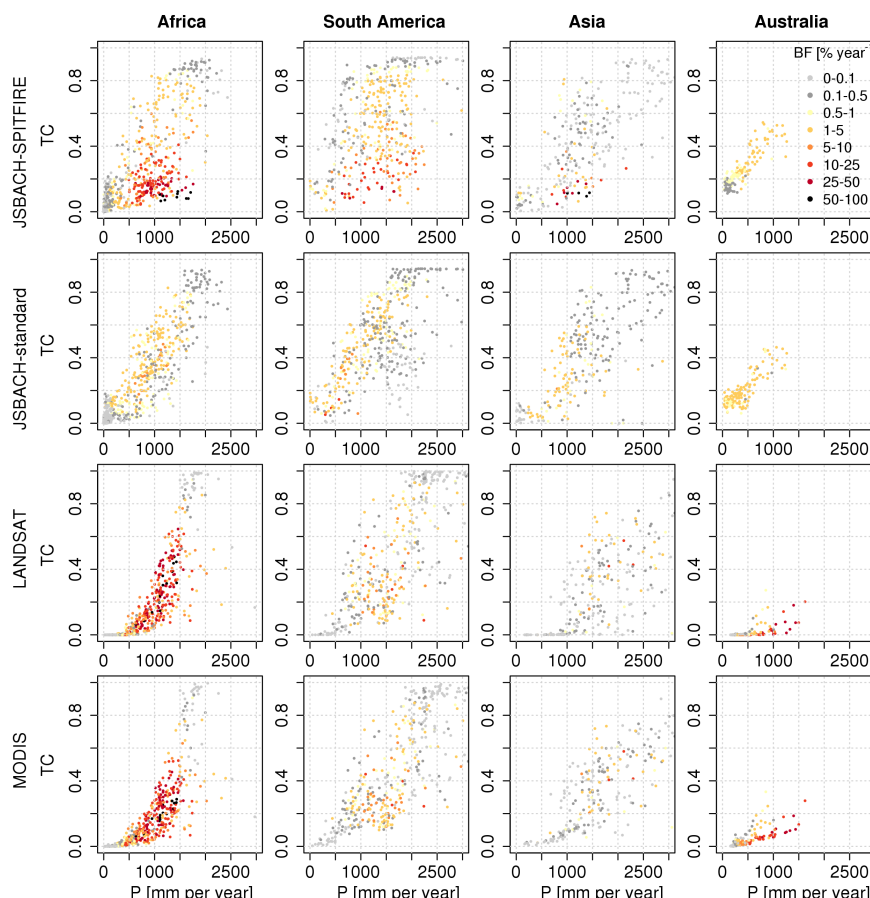


Figure 4. Modelled and observed tree cover (TC) versus precipitation (P), color coded burned area fraction (BF). Satellite datasets were aggregated to model grid resolution (1.875°).

ability of water and is therefore sensitive to drought. The establishment time scale of trees, however, is a constant (30 years for tropical PFTs) and only if a 5 year average of NPP turns negative, drought effects on the dynamic vegetation take effect. Other models require a minimum of 100 mm year^{-1} precipitation for sapling establishment (Sitch et al., 2003). The too high tree cover could be partly improved by improving the non-vegetated fraction which decreases too fast with increasing precipitation.

- 5 The too high dominance of trees (Figure 5) however indicates that the tree-grass competition is not well represented in the model. Tree-grass competition for water could for example be improved in the model by introducing the sapling stage of trees, which are competitively inferior to grasses (D’Onofrio et al., 2015).

The absence of fire for closed canopies is captured well by JSBACH-SPITFIRE, the modelled strong relationship between higher burned fraction and lower tree cover for open canopies, however, is not found in the observations. Inclusion or improve-

- 10 ment of several ecological processes might improve the modelled relationship. The adaptation of trees to frequent fires by

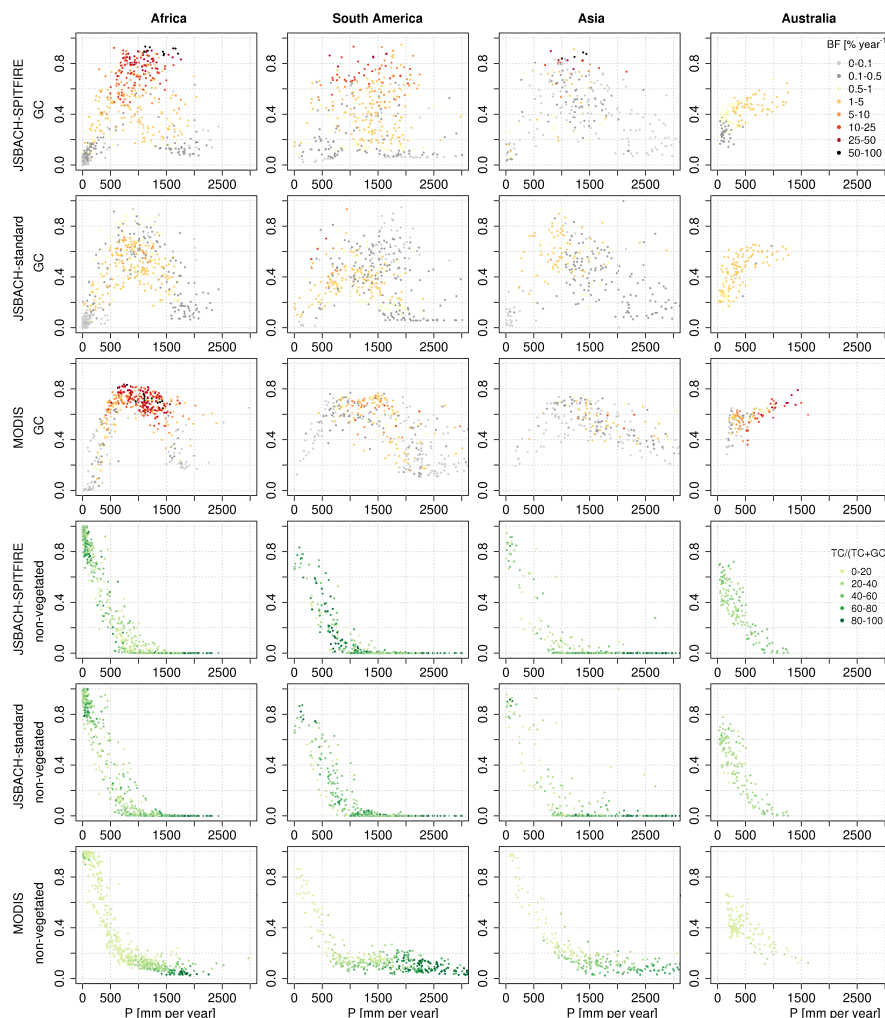


Figure 5. Modelled and observed grass cover (GC) and non-vegetated fraction over precipitation (P), with color coded burned area fraction (BF) for the grass cover and dominance of trees as (TC/total vegetation cover) for the non-vegetated fraction.

increased bark thickness, and therefore higher resistance of trees to fire (Pellegrini et al., 2017) would increase the tree cover in regions with high burned fraction. A second option could be a negative feedback between fire occurrence and tree mortality: frequent fire occurrence leads to low fuel loads and low fuel loads allow only low intensity fires with associated lower mortality of trees. This feedback is included in the SPITFIRE model, but might be too weak. A more detailed representation of vegetation structure including a sapling state of trees that is more sensitive to fire (e.g. Higgins et al., 2000) and a long lived adult tree state could increase the survival of trees.

For Australia underestimation of burned area for both fire models is strong. In a previous evaluation where the model was forced with observed climate and vegetation cover was prescribed (in contrast to the dynamic vegetation cover and climate

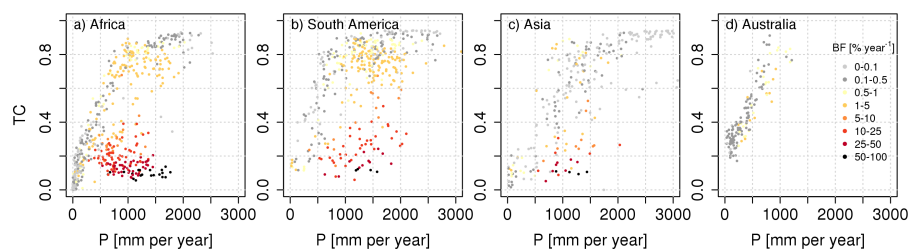


Figure 6. Same as Figure 4 for JSBACH-SPITFIRE but with preindustrial land use.

modelled by the MPI-ESM) JSBACH-SPITFIRE showed better results for Australia (Hantson et al., 2015). An improved response of vegetation cover dynamics to precipitation will therefore likely improve the patterns of burned area.

The rank correlation between precipitation and tree cover is higher for the observations compared to the model outputs. One reason might be the lower maximum tree cover for low precipitation in the observations which limits the range of tree cover values in these regions. In JSBACH-standard the correlation between tree cover and precipitation is stronger than in JSBACH-SPITFIRE. In the JSBACH-standard model, fire is only driven by meteorological variables and vegetation properties (which also largely follow climatic gradients). JSBACH-SPITFIRE, however, also uses population density and lightning datasets as input, which are potentially inconsistent with the meteorological forcing derived from the MPI-ESM output. This decoupling between climate and ignitions might cause the lower correlation for JSBACH-SPITFIRE compared to the JSBACH-standard simulation. For instance in the Northeast Amazon region precipitation of the MPI-ESM is too low, leading to a decrease in tree cover in regions with closed canopy with the JSBACH-standard fire model. The very low ignitions in JSBACH-SPITFIRE in that region contribute to a low fire occurrence compared to JSBACH-standard and in consequence to higher tree cover (Figure 1). Lightning can be computed within climate models (Krause et al., 2014) and using these lightning datasets based on the model not on observations would ensure consistency between meteorological forcing and the ignitions used in the fire model (Felsberg et al., 2018).

4.2 Difference between continents

We find differences in the climate-vegetation-fire relationships between continents in the satellite products as well as in the model simulations with JSBACH-SPITFIRE and the JSBACH standard model. Differences in the climate-vegetation-fire relationships have been described based on site level datasets (Lehmann et al., 2014). They find that the response of tree basal area to growth conditions (climate and nutrients) and disturbances differs between continents. The study suggests that the one climate–one vegetation paradigm which is an under-pinning of many global vegetation models cannot lead to vegetation patterns that differ between continents under the same climatic conditions as the patterns depend on past environmental conditions and evolution. Evolution is not accounted for in common vegetation models. In simulations with changing climatic forcing, however, the vegetation is a function of previous environmental conditions and adapts to changes in climate with usually PFT



specific time scales. Additionally the human dimension is more and more included in DGVMs, primarily by including anthropogenic land cover change. Moreover, in recent global fire models population density is a commonly used driver (Hantson et al., 2016). Our model simulations show that also the modelled climate-vegetation-fire relationships differ between continents. The simulations show a saturation in tree cover for higher precipitation for Africa, South America and Asia, but a linear increase for Australia. Site level observations show the same difference for tree basal area and effective rainfall (Lehmann et al., 2014). In the model this difference is not affected by land use and not by the type of fire model, it is therefore rather a result of different climate, maybe seasonality that is not resolved by the mean annual precipitation.

We confirmed in the factorial simulation that land cover change is influencing the differences in the modelled fire regime between Africa and South America. Land cover change influences simulated fire occurrence as cropland areas are excluded from burning and pastures have a higher fuel bulk density in the JSBACH-SPITFIRE model. A reduction in fire occurrence due to increases in croplands is well supported by statistical analysis of satellite data for Africa (Andela and van der Werf, 2014) and globally (Bistinas et al., 2014; Andela et al., 2017). The mechanism behind the reduction due to croplands is however likely a fragmentation of the landscape, which is not explicitly accounted for in the model.

Vegetation in the MPI Earth system model including SPITFIRE is not only a function of climate but also depends on the history of previous vegetation due to the feedback between fire and vegetation (Lasslop et al., 2016). We did not isolate the effect of the multi-stability in this study but initialized the model with the standard vegetation initialization of the MPI-ESM for the year 1850. The SPITFIRE model also takes into account differences in the fire regime through spatially varying ignitions. In addition to the effect of land use on the differences between continents these differences in ignitions might be important and might explain the smaller differences for the purely climate and land use driven JSBACH-standard model.

4.3 Limitations in the comparability between observations and modeled variables

We use two remotely sensed tree cover products, which show coherent patterns. Although these products are derived from imagery with different spectral, temporal and spatial characteristics (MODIS and Landsat), they cannot be considered totally independent because both are derived using a similar classification and regression tree method as well as reference data. The observational tree cover datasets are limited to trees taller than 5 m and do not include shrubs. For the model however we included shrubs and all trees. Previously differences in the threshold where maximum tree cover is reached were attributed to different precipitation datasets and ex- or inclusion of shrub cover (Devine et al., 2017). Filtering modelled and observed tree cover based on the presence of shrubs in the MODIS land cover product leads to only small differences in the relationship between tree cover and precipitation (Figure A1). Excluding grid cells where biomass indicates that the vegetation height is smaller than 5 m according to the allometric relationship used in SPITFIRE-JSBACH (Lasslop et al., 2014) did not lead to substantially different relationships (Figure A2). Our conclusions are therefore not affected by the limitation of the datasets to observe only trees taller than 5 m.

Compared to the satellite datasets, an African site level dataset shows lower thresholds of precipitation for the absence of trees (ca. 100 mm year⁻¹) and for reaching the highest tree cover values (>650 mm year⁻¹) (Sankaran et al., 2005). However, the general absence of trees for very low precipitation and increase until a certain threshold is similar to the remote sensing



datasets.

The maximum value of a variable can decrease due to spatial averaging. We tested this effect by not using the mean when aggregating the satellite tree cover to the resolution of the precipitation dataset but instead using the maximum value of the underlying 0.05° grid cells of tree cover. Canopy closure can then be reached for all continents for mean precipitation values around 500-1000 mm year⁻¹ (Figure A3), which is more consistent with a published site level dataset (Sankaran et al., 2005). This is consistent with the figures in Hirota et al. (2011) where the MODIS tree cover is shown in 1km resolution. The scale at which maximum tree covers are observed and the spatial scale of the model application therefore needs to be considered. Tree cover seems to be a clearly defined variable, but already varies between the two satellite datasets, the MODIS tree cover dataset defines a maximum tree cover of 80%, while the LANDSAT tree cover dataset allows a cover of 100%. In the model, tree cover and biomass are two rather independent variables, meaning that tree cover can be high in spite of a low biomass. In the observations not fully closed canopies due to low foliar biomass might be tracked as a reduced tree cover. Biomass datasets might therefore give additional valuable insights.

5 Conclusions

This study combines two satellite datasets with model simulations using a simple and a complex fire algorithm to investigate relationships between fire, vegetation and climate. Our analysis shows that the two satellite datasets are consistent in terms of the relationship between tree cover, precipitation and fire occurrence, but the spatial scale needs to be considered as some statistical characteristics change with the resolution.

Our analysis showed the strength of the multivariate comparison to detect model inconsistencies and guide model development. It goes beyond the insights gained by standard spatial comparisons. For JSBACH we find an overestimation of tree cover for low precipitation where typically fire occurrence is low due to limited fuel availability. The response of burned area to precipitation was captured well for SPITFIRE, but the simple fire scheme showed an overestimation of burned area for dry regions. This indicates that improved modelling of drought effects on the vegetation dynamics will improve the response of vegetation to climate in dry regions. Dry regions often show a strong coupling between land and atmosphere (Koster et al., 2006), such an improvement has therefore also a high potential to improve the performance of the coupled Earth system model.

While fire occurrence and vegetation patterns are well observed by remote sensing, the impact of fire on vegetation is much less constrained by satellite observations limiting the possibilities of evaluating that part of fire models. The multivariate comparison helped to identify a too strong effect of fire on tree cover, adaptation of trees to fire by increasing bark thickness or a stronger negative feedback between fire occurrence and fuel load are possible model improvements.

The complex fire model SPITFIRE improves the difference in fire regimes between the continents, especially Africa and South America, compared to the simple fire model. The factorial model simulation shows that anthropogenic land use contributes to differences in burned area between the continents in the JSBACH-SPITFIRE model. Our finding that models do show differences in the fire-vegetation-climate relationships between continents shows that although known variations in vegetation

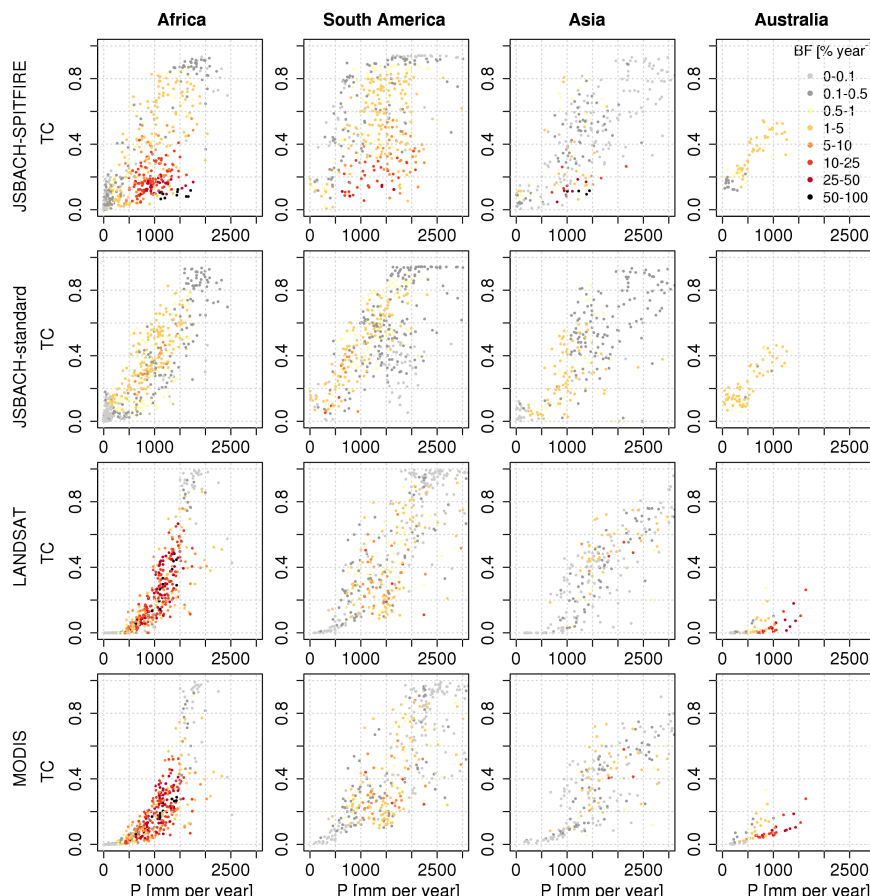


Figure A1. Same as figure 4 but tree cover filtered for the presence of shrub lands (using the MODIS open and closed shrub land classification). This indicates a low sensitivity of the fire-vegetation-climate relationships to shrub lands.

characteristics are not represented in models, they can be helpful to better understand intercontinental differences.

Code and data availability. The observational datasets are freely available. The processed data and model output as displayed in this publication and the processing scripts are available upon request to publications@mpimet.mpg.de.

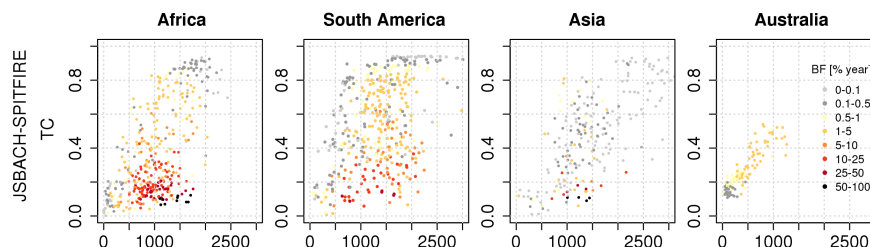


Figure A2. Modelled tree cover (TC) versus precipitation (P) [mm year⁻¹]. Modelled tree cover was filtered for vegetation height of trees <5 m using the modelled vegetation height. This value is given as detection threshold for the satellite products. When filtering the model output with this threshold the differences to the unfiltered dataset are very small (compare with Figure 4, panels for JSBACH-SPITFIRE).

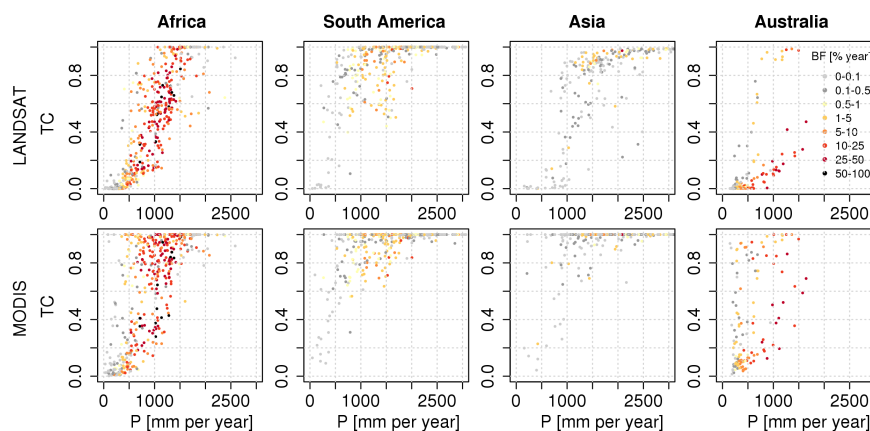


Figure A3. Tree cover (TC) versus precipitation (P) with color coded burned fraction (BF). Tree cover was here remapped from 0.05° resolution to 2° using the maximum value of the higher resolution instead of the mean.

Appendix A: Sensitivity of climate-vegetation-fire relationships to remapping, presence of shrubs and modelled tree height

Author contributions. GL and TM designed the study

Competing interests. The authors have no competing interests



Acknowledgements. We would like to thank the DKRZ for excellent computing facilities. D. D’Onofrio acknowledges support from the European Union Horizon 2020 research and innovation programme under grant agreement No 641816 (CRESCENDO). S.H. acknowledges support by the EU FP7 projects BACCHUS (grant agreement no. 603445) and LUC4C (grant agreement no. 603542). We thank Victor Brovkin for valuable discussions and comments on this manuscript.



References

- Alkama, R. and Cescatti, A.: Biophysical climate impacts of recent changes in global forest cover, *Science* (80-.), 351, 600–604, <https://doi.org/10.1126/science.aac8083>, <http://www.sciencemag.org/cgi/doi/10.1126/science.aac8083>, 2016.
- Andela, N. and van der Werf, G. R.: Recent trends in African fires driven by cropland expansion and El Niño to La Niña transition, *Nat. Clim. Chang.*, 4, 791–795, <https://doi.org/10.1038/nclimate2313>, <http://www.nature.com/doi/10.1038/nclimate2313>, 2014.
- 5 Andela, N., Morton, D. C., Giglio, L., Chen, Y., van der Werf, G. R., Kasibhatla, P. S., DeFries, R. S., Collatz, G. J., Hantson, S., Kloster, S., Bachelet, D., Forrest, M., Lasslop, G., Li, F., Mangeon, S., Melton, J. R., Yue, C., and Randerson, J. T.: A human-driven decline in global burned area, *Science* (80-.), 356, 1356–1362, <http://science.sciencemag.org/content/356/6345/1356.abstract>, 2017.
- Bathiany, S., Claussen, M., Brovkin, V., Raddatz, T., and Gayler, V.: Combined biogeophysical and biogeochemical effects of large-scale forest cover changes in the MPI earth system model, *Biogeosciences*, 7, 1383–1399, <https://doi.org/10.5194/bg-7-1383-2010>, <http://www.biogeosciences.net/7/1383/2010/>, 2010.
- 10 Baudena, M., Dekker, S. C., van Bodegom, P. M., Cuesta, B., Higgins, S. I., Lehsten, V., Reick, C. H., Rietkerk, M., Scheiter, S., Yin, Z., Zavala, M. A., and Brovkin, V.: Forests, savannas, and grasslands: bridging the knowledge gap between ecology and Dynamic Global Vegetation Models, *Biogeosciences*, 12, 1833–1848, <https://doi.org/10.5194/bg-12-1833-2015>, <http://www.biogeosciences.net/12/1833/2015/>, 2015.
- 15 Bistinas, I., Harrison, S. P., Prentice, I. C., and Pereira, J. M. C.: Causal relationships versus emergent patterns in the global controls of fire frequency, *Biogeosciences*, 11, 5087–5101, <https://doi.org/10.5194/bg-11-5087-2014>, 2014.
- Bonan, G. B.: Forests and climate change: forcings, feedbacks, and the climate benefits of forests., *Science* (80-.), 320, 1444–9, <https://doi.org/10.1126/science.1155121>, <http://www.ncbi.nlm.nih.gov/pubmed/18556546>, 2008.
- 20 Brovkin, V., Claussen, M., Petoukhov, V., and Ganopolski, A.: On the stability of the atmosphere-vegetation system in the Sahara/Sahel region, *J. Geophys. Res.*, 103, 31 613, <https://doi.org/10.1029/1998JD200006>, <http://doi.wiley.com/10.1029/1998JD200006>, 1998.
- Brovkin, V., Raddatz, T., Reick, C. H., Claussen, M., and Gayler, V.: Global biogeophysical interactions between forest and climate, *Geophys. Res. Lett.*, 36, 1–6, <https://doi.org/10.1029/2009GL037543>, <http://www.agu.org/pubs/crossref/2009/2009GL037543.shtml>, 2009.
- Devine, A. P., McDonald, R. A., Quaipe, T., and Maclean, I. M. D.: Determinants of woody encroachment and cover in African savannas, *Oecologia*, 183, 939–951, <https://doi.org/10.1007/s00442-017-3807-6>, <http://link.springer.com/10.1007/s00442-017-3807-6>, 2017.
- 25 D’Onofrio, D., Baudena, M., D’Andrea, F., Rietkerk, M., and Provenzale, A.: Tree-grass competition for soil water in arid and semiarid savannas: The role of rainfall intermittency, *Water Resour. Res.*, 51, 169–181, <https://doi.org/10.1002/2014WR015515>, <http://doi.wiley.com/10.1002/2014WR015515>, 2015.
- Felsberg, A., Kloster, S., Wilkenskeld, S., Krause, A., and Lasslop, G.: Lightning Forcing in Global Fire Models: The Importance of Temporal Resolution, *J. Geophys. Res. Biogeosciences*, <https://doi.org/10.1002/2017JG004080>, <http://doi.wiley.com/10.1002/2017JG004080>, 2018.
- 30 Friedl, M. A., Sulla-Menashe, D., Tan, B., Schneider, A., Ramankutty, N., Sibley, A., and Huang, X.: MODIS Collection 5 global land cover: Algorithm refinements and characterization of new datasets, *Remote Sens. Environ.*, 114, 168–182, <https://doi.org/10.1016/j.rse.2009.08.016>, <http://linkinghub.elsevier.com/retrieve/pii/S0034425709002673>, 2010.
- 35 Gerard, F., Hooftman, D., van Langevelde, F., Veenendaal, E., White, S. M., and Lloyd, J.: MODIS VCF should not be used to detect discontinuities in tree cover due to binning bias. A comment on Hanan et al. (2014) and Staver and Hansen (2015), *Glob. Ecol. Biogeogr.*, 26, 854–859, <https://doi.org/10.1111/geb.12592>, <http://dx.doi.org/10.1111/geb.12592>, 2017.



- Giglio, L., Randerson, J. T., and van der Werf, G. R.: Analysis of daily, monthly, and annual burned area using the fourth-generation global fire emissions database (GFED4), *J. Geophys. Res. Biogeosciences*, 118, 317–328, <https://doi.org/10.1002/jgrg.20042>, <http://doi.wiley.com/10.1002/jgrg.20042>, 2013.
- Giorgetta, M. A., Jungclaus, J., Reick, C. H., Legutke, S., Bader, J., Böttinger, M., Brovkin, V., Crueger, T., Esch, M., Fieg, K., Glushak, K., Gayler, V., Haak, H., Hollweg, H.-D., Ilyina, T., Kinne, S., Kornbluh, L., Matei, D., Mauritsen, T., Mikolajewicz, U., Mueller, W., Notz, D., Pithan, F., Raddatz, T., Rast, S., Redler, R., Roeckner, E., Schmidt, H., Schnur, R., Segschneider, J., Six, K. D., Stockhause, M., Timmreck, C., Wegner, J., Widmann, H., Wieners, K.-H., Claussen, M., Marotzke, J., and Stevens, B.: Climate and carbon cycle changes from 1850 to 2100 in MPI-ESM simulations for the Coupled Model Intercomparison Project phase 5, *J. Adv. Model. Earth Syst.*, 5, 572–597, <https://doi.org/10.1002/jame.20038>, <http://doi.wiley.com/10.1002/jame.20038>, 2013.
- 10 Hagemann, S., Loew, A., and Andersson, A.: Combined evaluation of MPI-ESM land surface water and energy fluxes, *J. Adv. Model. Earth Syst.*, pp. n/a–n/a, <https://doi.org/10.1029/2012MS000173>, <http://doi.wiley.com/10.1029/2012MS000173>, 2013.
- Hansen, M. C., DeFries, R. S., Townshend, J. R. G., Carroll, M., Dimiceli, C., and Sohlberg, R. a.: Global Percent Tree Cover at a Spatial Resolution of 500 Meters: First Results of the MODIS Vegetation Continuous Fields Algorithm, *Earth Interact.*, 7, 1–15, [https://doi.org/10.1175/1087-3562\(2003\)007<0001:GPTCAA>2.0.CO;2](https://doi.org/10.1175/1087-3562(2003)007<0001:GPTCAA>2.0.CO;2), [http://journals.ametsoc.org/doi/abs/10.1175/1087-3562\(2003\)007{ }3C0001:GPTCAA{ }3E2.0.CO;2](http://journals.ametsoc.org/doi/abs/10.1175/1087-3562(2003)007{ }3C0001:GPTCAA{ }3E2.0.CO;2), 2003.
- 15 Hansen, M. C., Potapov, P. V., Moore, R., Hancher, M., Turubanova, S. a., Tyukavina, A., Thau, D., Stehman, S. V., Goetz, S. J., Loveland, T. R., Kommareddy, A., Egorov, A., Chini, L., Justice, C. O., and Townshend, J. R. G.: High-resolution global maps of 21st-century forest cover change., *Science*, 342, 850–3, <https://doi.org/10.1126/science.1244693>, <http://www.ncbi.nlm.nih.gov/pubmed/24233722>, 2013.
- Hanson, S., Lasslop, G., Kloster, S., and Chuvieco, E.: Anthropogenic effects on global mean fire size, *Int. J. Wildl. Fire*, 24, 589–596, <https://doi.org/10.1071/WF14208>, <http://www.publish.csiro.au/?paper=WF14208>, 2015.
- 20 Hanson, S., Arneeth, A., Harrison, S. P., Kelley, D. I., Prentice, I. C., Rabin, S. S., Archibald, S., Mouillot, F., Arnold, S. R., Artaxo, P., Bachelet, D., Ciais, P., Forrest, M., Friedlingstein, P., Hickler, T., Kaplan, J. O., Kloster, S., Knorr, W., Lasslop, G., Li, F., Mangeon, S., Melton, J. R., Meyn, A., Sitch, S., Spessa, A., van der Werf, G. R., Voulgarakis, A., and Yue, C.: The status and challenge of global fire modelling, *Biogeosciences Discuss.*, pp. 1–30, <https://doi.org/10.5194/bg-2016-17>, <http://www.biogeosciences-discuss.net/bg-2016-17/>, 2016.
- 25 Higgins, S. I. and Scheiter, S.: Atmospheric CO₂ forces abrupt vegetation shifts locally, but not globally, *Nature*, 488, 209–212, <https://doi.org/10.1038/nature11238>, <http://www.nature.com/doi/10.1038/nature11238>, 2012.
- Higgins, S. I., Bond, W. J., and Trollope, W. S. W.: Fire, resprouting and variability: a recipe for grass–tree coexistence in savanna, *J. Ecol.*, 88, 213–229, <https://doi.org/10.1046/j.1365-2745.2000.00435.x>, <http://dx.doi.org/10.1046/j.1365-2745.2000.00435.x>, 2000.
- 30 Hirota, M., Holmgren, M., Van Nes, E. H., and Scheffer, M.: Global Resilience of Tropical Forest and Savanna to Critical Transitions, *Science* (80-.), 334, 232–235, <https://doi.org/10.1126/science.1210657>, <http://www.sciencemag.org/cgi/doi/10.1126/science.1210657>, 2011.
- Huffman, G., Adler, R., Bolvin, D., and Nelkin, E.: The TRMM Multi-satellite Precipitation Analysis (TMPA), in: *Satell. Rainfall Appl. Surf. Hydrol.*, edited by Hossain, F. and Gebremichael, M., chap. 1, pp. 3–22, Springer Verlag, 2010.
- Huffman, G. J., Bolvin, D. T., Nelkin, E. J., Wolff, D. B., Adler, R. F., Gu, G., Hong, Y., Bowman, K. P., and Stocker, E. F.: The TRMM Multisatellite Precipitation Analysis (TMPA): Quasi-Global, Multiyear, Combined-Sensor Precipitation Estimates at Fine Scales, *J. Hydrometeorol.*, 8, 38–55, <https://doi.org/10.1175/JHM560.1>, <http://journals.ametsoc.org/doi/abs/10.1175/JHM560.1>, 2007.
- Hurt, G. C., Chini, L. P., Froking, S., Betts, R. A., Feddema, J., Fischer, G., Fisk, J. P., Hibbard, K., Houghton, R. A., Janetos, A., Jones, C. D., Kindermann, G., Kinoshita, T., Klein Goldewijk, K., Riahi, K., Shevliakova, E., Smith, S., Stehfest, E., Thomson, A., Thornton, P.,



- Vuuren, D. P., and Wang, Y. P.: Harmonization of land-use scenarios for the period 1500–2100: 600 years of global gridded annual land-use transitions, wood harvest, and resulting secondary lands, *Clim. Change*, 109, 117–161, <https://doi.org/10.1007/s10584-011-0153-2>, <http://link.springer.com/10.1007/s10584-011-0153-2>, 2011.
- Klein Goldewijk, K., Goldewijk, K. K., and Klein Goldewijk, K.: Estimating global land use change over the past 300 years, *Glob. Biogeochem. Cycles*, 15, 417–43, <http://apps.isiknowledge.com/full{ }record.do?product=UA{ }search{ }mode=GeneralSearch{ }qid=3{ }SID=U2iG6akdAIElMenmoPf{ }page=1{ }doc=2{ }colname=WOS>, 2001.
- Kloster, S., Mahowald, N. M., Randerson, J. T., Thornton, P. E., Hoffman, F. M., Levis, S., Lawrence, P. J., Feddema, J. J., Oleson, K. W., and Lawrence, D. M.: Fire dynamics during the 20th century simulated by the Community Land Model, *Biogeosciences*, 7, 1877–1902, <http://www.biogeosciences.net/7/1877/2010/>, 2010.
- 10 Koster, R. D., Sud, Y. C., Guo, Z., Dirmeyer, P. A., Bonan, G., Oleson, K. W., Chan, E., Verseghy, D., Cox, P., Davies, H., Kowalczyk, E., Gordon, C. T., Kanae, S., Lawrence, D., Liu, P., Mocko, D., Lu, C.-H., Mitchell, K., Malyshev, S., McAvaney, B., Oki, T., Yamada, T., Pitman, A., Taylor, C. M., Vasic, R., and Xue, Y.: GLACE: The Global Land–Atmosphere Coupling Experiment. Part I: Overview, *J. Hydrometeorol.*, 7, 590–610, <https://doi.org/10.1175/JHM510.1>, <http://journals.ametsoc.org/doi/abs/10.1175/JHM510.1>, 2006.
- Krause, A., Kloster, S., Wilkenskield, S., and Paeth, H.: The sensitivity of global wildfires to simulated past, present, and future lightning frequency, *J. Geophys. Res. Biogeosciences*, 119, 312–322, <https://doi.org/10.1002/2013JG002502>, <http://doi.wiley.com/10.1002/2013JG002502>, 2014.
- 15 Krawchuk, M. a. and Moritz, M. a.: Constraints on global fire activity vary across a resource gradient., *Ecology*, 92, 121–32, <http://www.ncbi.nlm.nih.gov/pubmed/21560682>, 2011.
- Lasslop, G. and Kloster, S.: Impact of fuel variability on wildfire emission estimates, *Atmos. Environ.*, 121, 93–102, <https://doi.org/10.1016/j.atmosenv.2015.05.040>, <http://linkinghub.elsevier.com/retrieve/pii/S1352231015301126>, 2015.
- Lasslop, G. and Kloster, S.: Human impact on wildfires varies between regions and with vegetation productivity, *Environ. Res. Lett.*, <https://doi.org/10.1088/1748-9326/aa8c82>, <http://iopscience.iop.org/article/10.1088/1748-9326/aa8c82>, 2017.
- Lasslop, G., Thonicke, K., and Kloster, S.: SPITFIRE within the MPI Earth system model: Model development and evaluation, *J. Adv. Model. Earth Syst.*, 6, 740–755, <https://doi.org/10.1002/2013MS000284>, <http://doi.wiley.com/10.1002/2013MS000284>, 2014.
- 25 Lasslop, G., Brovkin, V., Reick, C. H., Bathiany, S., and Kloster, S.: Multiple stable states of tree cover in a global land surface model due to a fire–vegetation feedback, *Geophys. Res. Lett.*, 43, 6324–6331, <https://doi.org/10.1002/2016GL069365>, <http://doi.wiley.com/10.1002/2016GL069365>, 2016.
- Lehmann, C. E. R., Anderson, T. M., Sankaran, M., Higgins, S. I., Archibald, S., Hoffmann, W. A., Hanan, N. P., Williams, R. J., Fensham, R. J., Felfili, J., Hutley, L. B., Ratnam, J., San Jose, J., Montes, R., Franklin, D., Russell-Smith, J., Ryan, C. M., Durigan, G., Hiernaux, P., Haidar, R., Bowman, D. M. J. S., and Bond, W. J.: Savanna Vegetation–Fire–Climate Relationships Differ Among Continents, *Science* (80-.), 343, 548–552, <https://doi.org/10.1126/science.1247355>, <http://www.sciencemag.org/cgi/doi/10.1126/science.1247355>, 2014.
- 30 Li, F., Bond-Lamberty, B., and Levis, S.: Quantifying the role of fire in the Earth system – Part 2: Impact on the net carbon balance of global terrestrial ecosystems for the 20th century, *Biogeosciences*, 11, 1345–1360, <https://doi.org/10.5194/bg-11-1345-2014>, <http://www.biogeosciences.net/11/1345/2014/>, 2014.
- 35 Li, F., Lawrence, D. M., and Bond-Lamberty, B.: Impact of fire on global land surface air temperature and energy budget for the 20th century due to changes within ecosystems, *Environ. Res. Lett.*, 12, 44 014, <http://stacks.iop.org/1748-9326/12/i=4/a=044014>, 2017.
- Moncrieff, G. R., Scheiter, S., Bond, W. J., and Higgins, S. I.: Increasing atmospheric CO₂ overrides the historical legacy of multiple stable biome states in Africa, *New Phytol.*, 201, 908–915, <https://doi.org/10.1111/nph.12551>, <http://doi.wiley.com/10.1111/nph.12551>, 2014.



- Pellegrini, A. F. A., Anderegg, W. R. L., Paine, C. E. T., Hoffmann, W. A., Kartzinel, T., Rabin, S. S., Sheil, D., Franco, A. C., and Pacala, S. W.: Convergence of bark investment according to fire and climate structures ecosystem vulnerability to future change, *Ecol. Lett.*, 20, 307–316, <https://doi.org/10.1111/ele.12725>, <http://doi.wiley.com/10.1111/ele.12725>, 2017.
- Prentice, I. C., Kelley, D. I., Foster, P. N., Friedlingstein, P., Harrison, S. P., and Bartlein, P. J.: Modeling fire and the terrestrial carbon balance, *Global Biogeochem. Cycles*, 25, 1–13, <https://doi.org/10.1029/2010GB003906>, <http://www.agu.org/pubs/crossref/2011/2010GB003906.shtml>, 2011.
- Rabin, S. S., Melton, J. R., Lasslop, G., Bachelet, D., Forrest, M., Hantson, S., Kaplan, J. O., Li, F., Mangeon, S., Ward, D. S., Yue, C., Arora, V. K., Hickler, T., Kloster, S., Knorr, W., Nieradzik, L., Spessa, A., Folberth, G. A., Sheehan, T., Voulgarakis, A., Kelley, D. I., Prentice, I. C., Sitch, S., Harrison, S., and Arneth, A.: The Fire Modeling Intercomparison Project (FireMIP), phase 1: experimental and analytical protocols with detailed model descriptions, *Geosci. Model Dev.*, 10, 1175–1197, <https://doi.org/10.5194/gmd-10-1175-2017>, <http://www.geosci-model-dev.net/10/1175/2017/>, 2017.
- Reick, C. H., Raddatz, T., Brovkin, V., and Gayler, V.: Representation of natural and anthropogenic land cover change in MPI-ESM, *J. Adv. Model. Earth Syst.*, 5, 459–482, <https://doi.org/10.1002/jame.20022>, <http://doi.wiley.com/10.1002/jame.20022>, 2013.
- Sankaran, M., Hanan, N. P., Scholes, R. J., Ratnam, J., Augustine, D. J., Cade, B. S., Gignoux, J., Higgins, S. I., Le Roux, X., Ludwig, F., Ardo, J., Banyikwa, F., Bronn, A., Bucini, G., Caylor, K. K., Coughenour, M. B., Diouf, A., Ekaya, W., Feral, C. J., February, E. C., Frost, P. G. H., Hiernaux, P., Hrabar, H., Metzger, K. L., Prins, H. H. T., Ringrose, S., Sea, W., Tews, J., Worden, J., and Zambatis, N.: Determinants of woody cover in African savannas., *Nature*, 438, 846–849, <https://doi.org/10.1038/nature04070>, 2005.
- Sitch, S., Smith, B., Prentice, I. C., Arneth, A., Bondeau, A., Cramer, W., Kaplan, J. O., Levis, S., Lucht, W., Sykes, M. T., Thonicke, K., and Venevsky, S.: Evaluation of ecosystem dynamics, plant geography and terrestrial carbon cycling in the LPJ dynamic global vegetation model, *Glob. Chang. Biol.*, 9, 161–185, <https://doi.org/10.1046/j.1365-2486.2003.00569.x>, <http://doi.wiley.com/10.1046/j.1365-2486.2003.00569.x>, 2003.
- Staver, A. C., Archibald, S., and Levin, S.: Tree cover in sub-Saharan Africa: Rainfall and fire constrain forest and savanna as alternative stable states, *Ecology*, 92, 1063–1072, <https://doi.org/10.1890/10-1684.1>, <http://www.esajournals.org/doi/10.1890/10-1684.1>, 2011a.
- Staver, A. C., Archibald, S., and Levin, S. A.: The Global Extent and Determinants of Savanna and Forest as Alternative Biome States, *Science* (80-.), 334, 230–232, <https://doi.org/10.1126/science.1210465>, <http://www.sciencemag.org/cgi/doi/10.1126/science.1210465>, 2011b.
- Stevens, B., Giorgetta, M., Esch, M., Mauritsen, T., Crueger, T., Rast, S., Salzmann, M., Schmidt, H., Bader, J., Block, K., Brokopf, R., Fast, I., Kinne, S., Kornbluh, L., Lohmann, U., Pincus, R., Reichler, T., and Roeckner, E.: Atmospheric component of the MPI-M Earth System Model: ECHAM6, *J. Adv. Model. Earth Syst.*, 5, 146–172, <https://doi.org/10.1002/jame.20015>, <http://doi.wiley.com/10.1002/jame.20015>, 2013.
- Townsend, J., Carroll, M., DiMiceli, C., Sohlberg, R., Hansen, M., and DeFries, R.: Vegetation Continuous Fields MOD44B, 2001-2010 Percent Tree Cover, Collection 5, Version 051, 2011.
- Xu, C., Hantson, S., Holmgren, M., van Nes, E. H., Staal, A., and Scheffer, M.: Remotely sensed canopy height reveals three pantropical ecosystem states, *Ecology*, 97, 2518–2521, <https://doi.org/10.1002/ecy.1470>, <http://doi.wiley.com/10.1002/ecy.1470>, 2016.
- Yin, Z., Dekker, S. C., van den Hurk, B. J. J. M., and Dijkstra, H. A.: Bimodality of woody cover and biomass across the precipitation gradient in West Africa, *Earth Syst. Dyn.*, 5, 257–270, <https://doi.org/10.5194/esd-5-257-2014>, <http://www.earth-syst-dynam.net/5/257/2014/>, 2014.



Yue, C., Ciais, P., Zhu, D., Wang, T., Peng, S. S., and Piao, S. L.: How have past fire disturbances contributed to the current carbon balance of boreal ecosystems?, *Biogeosciences*, 13, 675–690, <https://doi.org/10.5194/bg-13-675-2016>, <https://www.biogeosciences.net/13/675/2016/>, 2016.